Eur Biophys J (2007) 36 (Suppl 1):S37–S48
DOI 10.1007/s00249-007-0174-y

THE EBSA PRIZE LECTURE

Magnetic resonance in the solid state: applications to protein folding, amyloid fibrils and membrane proteins

Marc Baldus

Received: 6 May 2007 / Accepted: 8 May 2007 / Published online: 31 May 2007

Abstract Solid-state nuclear magnetic resonance (ssNMR) represents a spectroscopic method to study non-crystalline molecules at atomic resolution. Advancements in spectroscopy and biochemistry provide increasing possibilities to study structure and dynamics of complex biomolecular systems by ssNMR. Here, methodological aspects and applications in the context of protein folding and aggregation are discussed. In addition, studies involving membrane proteins are considered.

Introduction

Nuclear magnetic resonance (NMR) spectroscopy probes the interaction of microscopic, nuclear magnetic moments (such as ^{1}H, ^{13}C, or ^{15}N spins) with a static magnetic field (B_0) and an external radio frequency (r.f.) field (Ernst et al. 1987). NMR has become the premier method to study structure and dynamics of molecules in solution including small ligands, globular and unfolded proteins [see, e.g., (Cavanagh 1996; Dyson and Wright 2004; Ernst et al. 1987; Wüthrich 1986)].

Solid-state NMR refers to applications where molecular size or chemical environment prohibit fast molecular tumbling in solution. As a result, the size and the orientation dependence of the nuclear spin interactions require the use of specialized instrumentation and methodology to study molecular structure and dynamics at atomic resolution. While such experiments are not influenced by protein size or the degree of structural order, applications in structural biology focused, for a long time, on the use of selectively labeled molecules and the application of 1D experiments. Under such conditions, the measurement of a single structural parameter was, for example, used to probe molecular motion in biomolecules or in the context of ligand–protein and protein–protein interactions [see, e.g., (Griffin 1981; McDowell and Schaefer 1996; Opella 1986; Palmer et al. 1996; Torchia 1984; Watts 2005)].

In the last years, several examples have appeared demonstrating that multiply- or uniformly isotope-labelled molecules can, in addition, increasingly be used to study molecular interactions on the atomic level (Baldus 2006; de Groot 2000; Griffin 1998; Hong 2006; McDermott 2004; Opella and Marassi 2004; Tycko 2006). Combined with recent methodological and instrumental progress in ssNMR, such studies not only can lead to the determination of entire 3D molecular structures but also offer a means for site-specific analysis, for example of the influence of molecular dynamics or the effect of molecular complex formation. In this contribution I will discuss recent results using ssNMR to study protein structure and dynamics in the context of amyloid fibrils and membrane proteins. In addition, novel approaches to investigate molecular folding by ssNMR will be considered. In all cases, applications will be conducted under high-resolution ssNMR, i.e., magic angle spinning (MAS) (Andrew et al. 1958) conditions.

Methods

Because magnetic resonance in the solid state does not require crystalline and soluble samples, experiments can be conducted under different preparatory conditions. Possible experimental preparations range from powders and frozen

M. Baldus (✉)
Solid-state NMR, Max-Planck-Institut für Biophysikalische Chemie, 37077 Göttingen, Germany
e-mail: maba@mpibpc.mpg.de

solutions to microcrystals, gels or proteoliposomes (Fig. 1). Working with multiply—or fully isotope-labeled molecules is a prerequisite if multiple structural constraints are to be deduced from a single ssNMR sample. Unless molecular size or mobility allow for the direct use of ^{1}H evolution and detection periods, a high degree of ^{13}C and ^{15}N isotope labelling is mandatory if molecular structure is to be investigated under MAS conditions. Depending on the application of interest, chemical synthesis, cell free or bacterial expression systems are employed. In the case of protein expression in cell cultures, uniform isotope labelling is easily achieved using uniformly labelled starting media such as uniformly ^{13}C labeled glucose and $^{15}NH_4Cl$. More advanced labelling patterns can be generated if specifically labelled precursors, amino acids or growth media are supplied. In the case of membrane proteins, the uniformly labelled protein of interest is subsequently reconstituted into model membranes which can be studied in liposomes, possibly macroscopically oriented on solid glass (Glaubitz and Watts 1998) or polymer supports (Andronesi et al. 2004; Sizun and Bechinger 2002).

The structural analysis then proceeds using a series of multi-dimensional correlation experiments. In a first stage, sequential resonance assignments can be generated using a combination of (^{13}C,^{15}N) (see e,g., Baldus 2002) and (^{13}C,^{13}C) (Seidel et al. 2004) correlation methods. Since backbone chemical shifts provide a sensitive means of local dihedral angle constraints (Wishart and Sykes 1994), these resonance assignments provide an easy and powerful instrument to assess polypeptide secondary structure. In addition to the conformation-dependent chemical shift ($\Delta\delta$, Fig. 2), distances (encoded as dipolar couplings d) can be used to refine the local polypeptide conformation in the solid state. For example, the backbone (H_α, H_N) distance between sequential residues strongly correlates with the backbone dihedral angle ψ and can easily be detected during a NHHC correlation experiment (Lange et al. 2002, 2003). Likewise, the sequential ^{15}N–^{15}N distance can be used to refine the backbone topology (Cross et al. 1983). Information about the backbone conformation in the solid state can also be obtained by correlating two anisotropic interactions such as the chemical shift anisotropy (CSA) or the dipolar coupling in a 2D experiment. Here, one exploits the defined orientation of dipolar tensors along the internuclear vector and empirical knowledge regarding the orientation of CSA tensors. These anisotropic interactions can be recoupled during the evolution and/or detection period of a homonuclear or heteronuclear 2D correlation experiment by appropriate radio frequency schemes. The resulting cross-peak pattern is characteristic for the relative orientation of the two anisotropic interactions (Ishii et al. 1996). In uniformly labeled peptides, correlations between NH/NH (Reif et al. 2000) and NH/CH (Rienstra et al. 2002) dipolar tensors have been used for backbone dihedral angle determinations. Alternatively, relative tensor orientation may be encoded in the evolution of a double-quantum (2Q) two-spin state under the effect of two anisotropic interactions. Applications correlating CH/NH (Hong et al. 1997) and CN/CN (Costa et al. 1997; Feng et al. 1997) dipolar couplings or sequential carbonyl CSAs (Blanco and Tycko 2001) have been demonstrated. In a 2Q correlation experiment under CN dipolar dephasing, the signal amplitude can

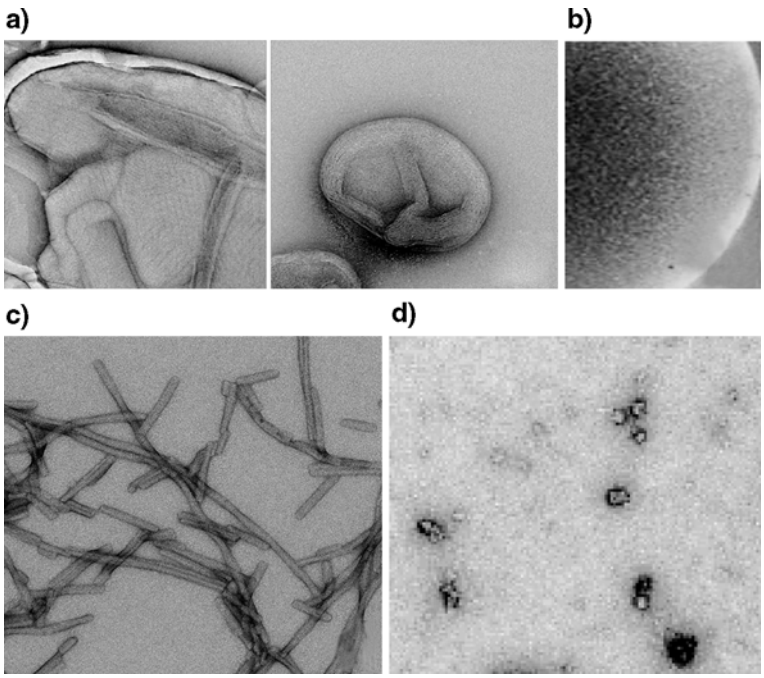

Fig. 1 Possible sample preparations for high-resolution solid-state NMR experiments (as seen by electron microscopy) range from proteoliposomes (**a**) and microcrystals (**b**) to protein fibrils (**c**) or molecular aggregates (**d**)

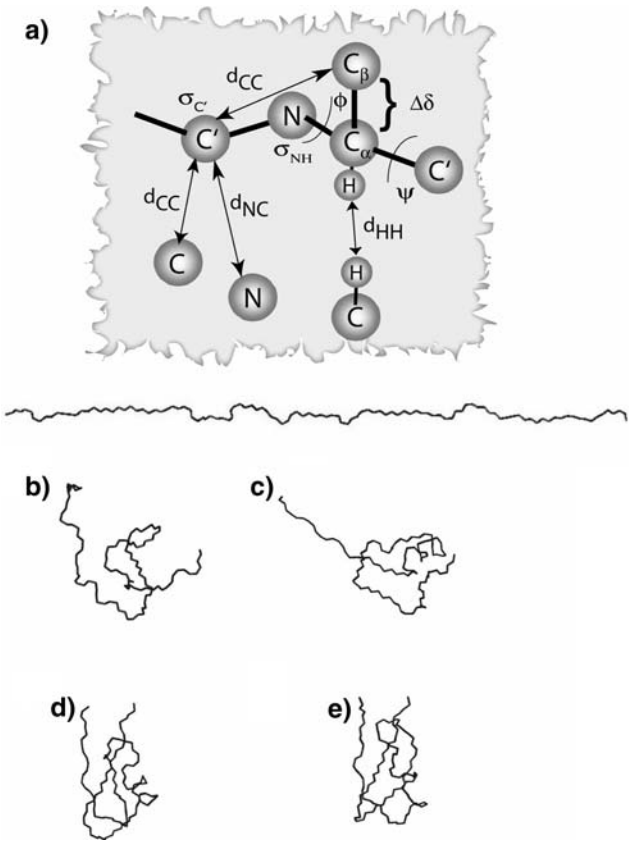

Fig. 2 Structural parameters to be detected in the context of MAS ss-NMR: in addition to the isotropic chemical shift (which can be used to define conformation-dependent chemical shifts $\Delta\delta$), anisotropic chemical shielding interactions (such as $\sigma_{C'}$, σ_{NH}) can be used to establish dihedral or other orientational constraints. In addition, distances (*d*) determine local and overall molecular 3D structure and can be measured by a variety of experimental methods. The combination of these parameters can be used to construct a 3D molecular structure from a single or a small set of isotope-labeled molecules under MAS conditions. In **a**–**e**, different stages of a structure calculation routine based on MAS–NMR data is exemplified for the case of Kaliotoxin [see ref. (Lange et al. 2005) and text for further details]

directly report on the backbone torsion angle and can hence conveniently be applied in multiply labeled polypeptides (Baldus 2002). In the case of severe spectral overlap, extensions to three spectral dimensions are possible (Heise et al. 2005c; Ladizhansky et al. 2003). All these experiments can help to establish local distance or torsion angle constraints that can be supplemented in a conventional structure calculation.

The 3D structure is finally determined if medium and long-range distance constraints can be derived from MAS NMR data. In the case of uniformly labelled molecules, the spin systems dynamics are dominated by one-bond (^{13}C,^{13}C) and (^{13}C,^{15}N) interactions. If spectral dispersion is favorable, selective (^{13}C,^{15}N) or (^{13}C,^{13}C) distance measurements can be performed in uniformly labelled peptides (Jaroniec et al. 2001; Nomura et al. 1999) and proteins (Sonnenberg et al. 2004). Moreover, isotope labelling schemes can be applied that lead to a partial dilution of the coupled (^{13}C,^{15}N) spin network. As a result, the influence of one-bond interactions is reduced and local (^{13}C,^{13}C) dipolar couplings can become comparable to medium and long-range interactions (Castellani et al. 2002). In addition, proton–proton distance restraints that provide the most abundant source of inter-residue interactions in the range up to 4 Å can be probed. For this purpose, indirect detection schemes are available that encode proton–proton polarization transfer in high-resolution ^{15}N and ^{13}C evolution and detection periods (i.e., NHHC and CHHC pulse schemes (Lange et al. 2002, 2003). Finally, orientational constraints can be established if anisotropic interactions such as NH CSA or dipolar tensor components are measured in macroscopically oriented systems. Under fast MAS, tailored r.f schemes that (Andronesi et al. 2004) recover anisotropic interactions can be used.

The details of a subsequent structure calculation are exemplified for the 38 amino acid polypeptide kaliotoxin (KTX, vide infra) in Fig. 2: first, an extended conformer is created (Fig. 2a) and subjected to simulated annealing protocol consisting of several stages. While in (Fig. 2b), three disulphide bonds are used as sole structural constraints, we have incorporated in (Fig. 2c) 65 dihedral angle restraints. As a result, secondary structure is formed but the overall 3D fold remains undefined. For this reason, proton–proton distance restraints are supplemented which relate to unequivocal spectral assignments in the first (D) or second round (E) of structure calculations. An ensemble of conformers with the lowest energy is finally reported. Further details of the structure calculation in the case of KTX are given in Lange et al. (2005).

To date, 3D structures of several crystalline and non-crystalline compounds have been obtained under MAS conditions. With the increasing possibilities to determine 3D molecular structures, the determination of site-resolved molecular dynamics of an entire polypeptide or (membrane) protein comes into reach. Such studies are particularly relevant for molecular segments in which structural constraints are missing or weak. Whenever motion is on the time scale of the inverse of the anisotropic interaction, such as the quadrupolar and dipolar interaction or the chemical shielding anisotropy, the measurement of the residual anisotropic interactions can be used to define a motion-based scaling parameter. In Fig. 3, the combined application of high-resolution solid-state NMR methods to a uniformly labeled biomolecule is exemplified for a small molecule: L-tyrosine–ethylester, TEE. Firstly, resonance assignments are obtained using a combination of (^{13}C,^{13}C) (and possibly ^{15}N,^{13}C) experiments (a). Subsequently, 2D experiments are used to collect structural constraints (here using a CHHC

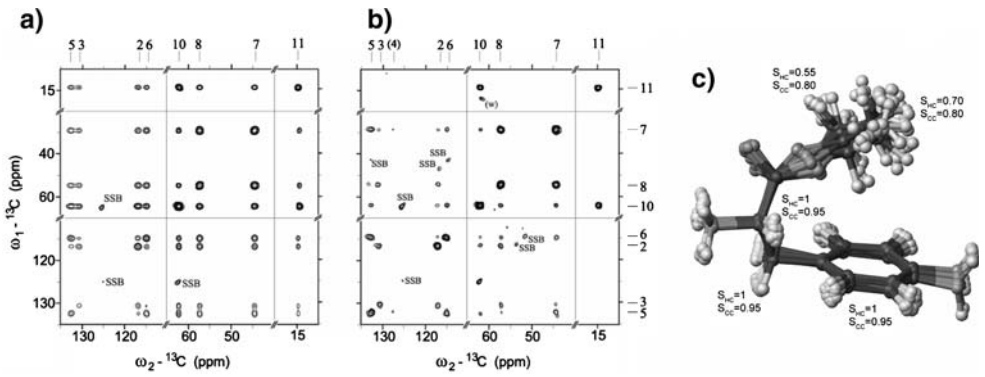

Fig. 3 The combined application of high-resolution ssNMR methods to uniformly labeled L-tyrosine-ethylester (TEE). Firstly, resonance assignments are obtained using a combination of (^{13}C,^{13}C) experiments (**a**). Subsequently, a 2D CHHC experiment (**b**) delivers (^{1}H,^{1}H) distance constraints resulting in the 3D structure of the molecule (**c**). In addition, local (^{1}H,^{13}C) or (^{13}C,^{13}C) order parameters $S < 1$ reflect molecular motion in the solid state. For details of the spin numbering, see (Seidel et al. 2005)

experiment, b) resulting in the 3D structure of the molecule. Finally, local motion can be studied by determining the residual one-bond (^{1}H,^{13}C) (Seidel et al. 2005) or (^{13}C,^{13}C) (Schneider et al. 2007) dipolar interaction (c). Note that in the case of TEE, the ester tail exhibits enhanced molecular motion [reflected by an order parameter $S < 1$ (Seidel et al. 2005; Schneider et al. 2007)] in the solid state. In the presence of faster molecular motion, dipolar-based transfer methods become inefficient and through-bond interactions invoking a combination of INEPT (Morris and Freeman 1979) and TOBSY (Baldus and Meier 1996) transfers can be applied (Andronesi et al. 2005). Such experiments have been applied to both proteoliposomes and fibril protein preparations (See Applications) and permit a spectral separation of protein signals based on local molecular mobility.

With the ability to separate signal components stemming from molecular segments with different local mobility, the measurement of domain sizes and molecular interfaces becomes feasible. Firstly, applications focused on individual protein segments, probing protein signals in one spectroscopic dimension (see, e.g., Kumashiro et al. 1998). More recently, advancements in spectroscopic sensitivity permit the recording of 2D correlations experiments in reference to a mobile ^{1}H environment. Again, applications can range from membrane proteins to biopolymers.

Applications

Amyloid proteins

Amyloid fibrils are β-sheet rich insoluble aggregates, which can be formed by almost all proteins and peptides independent of their primary sequence (Dobson 2002). A structural motif common to all amyloid fibrils is the cross-β pattern characterized by β-sheets parallel to the fibril axis with the strands perpendicular to the main axis (Serpell et al. 2000; Sunde et al. 1997). The deposition of amyloid aggregates is linked to many neurodegenerative diseases, such as Parkinson's and Alzheimer's disease (Caughey and Lansbury 2003). Since protein fibrils are—unless consisting of short model peptides (Makin et al. 2005; Nelson et al. 2005)—intrinsically non-crystalline and insoluble, ssNMR has emerged as the method of choice for structural studies on amyloid fibrils (Chan et al. 2005; Chimon and Ishii 2005; Ferguson et al. 2006; Heise et al. 2005a; Iwata et al. 2006; Jaroniec et al. 2004; Petkova et al. 2002, 2004, 2005, 2006; Ritter et al. 2005; Shewmaker et al. 2006; Siemer et al. 2006; Tycko 2004; vanderWel et al. 2006).

Measurements performed on Aβ amyloid peptides suggested that the supramolecular structure depends on the exact length of the particular peptide sequence (see, e.g., Tycko 2004 and references therein) and that different fibril morphologies have different underlying molecular structures correlated with different neuronal toxicities (Petkova et al. 2005). For this reason, we have, for example, studied fibril formation using full length constructs (i.e., 140 aa's) of α-synuclein related to Parkinson's disease. α-synuclein fibrils are the main component of protein aggregates associated with the loss of functionality of dopaminergic neurons in the context of Parkinson's disease. The 140 amino acid protein α-synuclein consists of an amphipathic N-terminus, a predominantly hydrophobic middle, so called NAC (non-Aβ component) region (residues 61–95), and a highly acidic and proline (P)-rich C terminus (residues 96–140). Apart from some long-range interactions (Bertoncini et al. 2005)—largely unfolded in its native state (Weinreb et al. 1996). Upon aggregation, a large fraction of α-synuclein undergoes a transition from random-coil structure to the cross-β conformation typical for amyloid fibrils (Conway et al. 2000; Serpell et al. 2000).

SsNMR studies of the full length constructs of α-synuclein are in general complicated by the chain length, the repetitiveness of amino acid motifs, and the difficulty to recombinantly produce isotope labeling at specific amino acid residues. Our spectroscopic analysis (Heise et al. 2005a) hence included the use of 3D correlation experiments, mobility filters and reverse isotope labeling schemes (Vuister et al. 1994) that simplified the ssNMR analysis. As a result, we could separate signal contributions arising from the rigid core of α-synuclein fibrils and resonances reflecting the mobile C-terminus of the fibrils or soluble monomers using through-space and through-bond correlation methods, respectively. The measurements led to the conclusion that α-synuclein fibrils contain a central region that is rich in β-strand segments, a highly flexible C terminus, and a disordered N terminus (Fig. 4). Variations in solid-state NMR spectra of different samples were found for the central β-strand region (Fig. 4 c, d), suggesting that at least two distinct fibril nucleation mechanisms exist for the formation of AS fibrils. The corresponding forms differ in terms of length of the observed β-strands. More recently, we have refined our structural analysis using H_2O-edited 2D correlation spectroscopy (Heise et al. 2007).

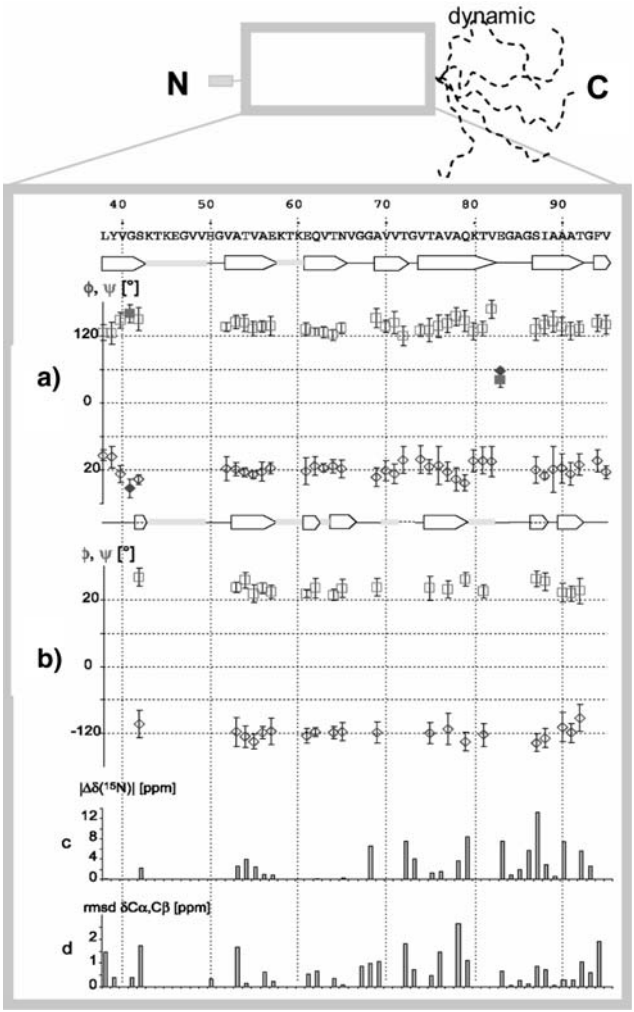

Fig. 4 Characterization of the core region (residues 38–95) of α-synuclein fibrils by solid-state NMR. While the central region is rich in β-strand segments [torsion angle constraints were obtained using a combination of chemical shift and (^{1}H,^{1}H) distance information (Heise et al. 2005a)], α-synuclein fibrils contain a highly flexible C terminus and a disordered N terminus. Variations in ssNMR ^{15}N and ^{13}Cα,β chemical shifts were found for the central β-strand region, suggesting that at least two distinct fibril nucleation mechanisms exist for the formation of α-synuclein fibrils

Molecular folding

In addition to the structural investigation of mature protein fibrils or biopolymers, ssNMR also provides a spectroscopic means to study protein folding in a residue-specific level or in real time. In a first set of experiments, we (and others Havlin and Tycko 2005) developed a strategy to monitor motional amplitudes of intrinsically disordered polypeptides from 2D ssNMR experiments. For example, this concept was applied to probe the residual structure of the neuropeptide neurotensin (NT) in an aqueous and lipid-bound state. To characterize the conformational space adopted by NT, we analyzed 2D ssNMR data (i.e., the correlation of conformation-dependent Cα and Cβ chemical shifts) obtained in the frozen state using a combination of molecular dynamics calculations and DFT-based methods (Heise et al. 2005b). Although this approach does not deliver a quantitative analysis of the NT structures in solution, it revealed a general propensity of the peptide to adopt extended conformations which, on the level of individual residues, is determined by hydrophobic character of the side chain. Notably, a recent solution-state NMR study of the free, full-length peptide is largely in accordance with our ssNMR analysis (Coutant et al. 2007).

Many folding events take place on the slow time scale. This aspect has prompted us to explore possibilities to record time-resolved ssNMR during protein folding. Pioneered for applications in soluble molecules (Balbach et al. 1996), such an approach recently allowed us to record spectroscopic 'footprints' (Etzkorn et al. 2007a) describing the refolding of a precipitated protein due to a slight temperature increase by 2D ssNMR. These studies not only demonstrated that high-resolution ssNMR spectra can be obtained from precipitated proteins (for a comparison between microcrystalline and precipitated samples, see Fig. 5) but also showed that a domain swapped protein does not necessarily refold into an aggregated structure in which the domain swapped interface is maintained. In a general sense, such studies should offer a means to study slow structural rearrangements and their kinetic profiles on a residue-specific level.

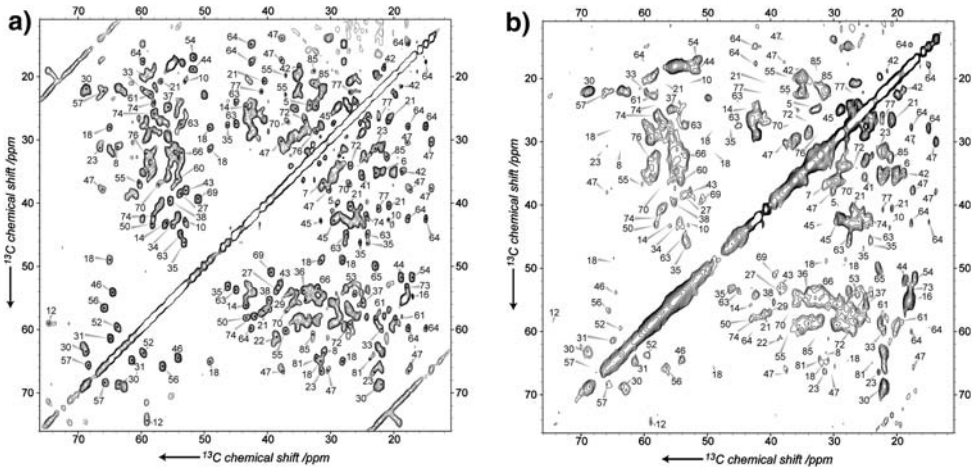

Fig. 5 Comparison of 2D ssNMR (^{13}C,^{13}C) correlation spectra obtained on isotope-labeled protein Crh [see e,g., (Böckmann et al. 2003)] in microcrystalline (**a**) and precipitated (**b**) form

Ligand–membrane protein interactions

For more than three decades, solid-state NMR (ssNMR) has been applied to the structural study of membranes and proteins associated with them. Probably, bacteriorhodopsin and rhodopsin represent the membrane proteins most extensively studied by MAS-based solid-state NMR methods (see, for example, Eilers et al. 2002; Herzfeld and Lansing 2002, for recent reviews). In addition to these retinal proteins, a variety of membrane embedded systems have been the subject of ssNMR-based structural studies, often involving macroscopically oriented systems (Cross and Opella 1994; Marassi and Opella 1998; Opella and Marassi 2004). In fact, several 3D structures of peptides embedded in oriented bilayers have been determined by solid-state NMR techniques (Opella and Marassi 2004). In addition, ssNMR has made considerable progress in probing ligand binding to membrane proteins. Such studies involved the determination of individual structural constraints from a specifically labeled biomolecule (see, e.g., Creuzet et al. 1991; Watts 1999, 2005) and, more recently, rely on the use of multiply or uniformly labeled samples (Creemers et al. 2002; Krabben et al. 2004; Patel et al. 2004).

Progress in high-field ssNMR instrumentation was crucial for our study of neurotensin bound its G-protein coupled receptor (Luca et al. 2003). Here, nanomolar quantities of the receptor could be produced by Grisshammer and Tucker (2000). The high affinity of the ligand to its receptor has thus far precluded the elucidation of the receptor-bound ligand conformation by solution-state NMR (see, for example, ref. Inooka et al. 2001). An NMR study in the presence of detergent reported NT(8–13) chemical shift changes upon receptor interaction (Williamson et al. 2002).

Studying the bioactive conformation of NT without signal overlap from excess (unbound) NT required the measurement µg quantities of the peptide (Luca et al. 2003). Notably, not only the full length peptide, but also the C-terminal part of neurotensin, NT(8–13), has been found to interact with NTS−1 with high affinity (see for example refs. Goedert 1989; Tanaka et al. 1990). Because of the limited sensitivity, our study focussed on the determination of conformation-dependent chemical shifts of the bioactive form of NT, i.e., NT(8–13). Nevertheless, this information was sufficient to build a low-resolution structural model of the peptide backbone (Fig. 6) in complex with the receptor and has lead to the synthesis of designed peptides that mimic the ssNMR-derived torsion angles (Luca et al. 2005). In addition, our ssNMR study may provide the basis for additional experiments determining distances or side-chain orientations of selectively-labeled peptide variants.

On the other hand, if sufficient protein quantities are available, it is possible to determine entire ligand structures, as we have recently demonstrated for the scorpion toxin Kaliotoxin in complex with a chimeric (KcsA-Kv1.3) ion channel (Lange et al. 2006). Kaliotoxin (KTX) is a 38-residue peptide (Fig. 7) found in the venom of the scorpion *Androctonus mauretanicus mauretanicus*. Binding of KTX (Legros et al. 2000, 2002) and KTX mutants to these K^+ channels is similar to the interaction of KTX with the Shaker-related T-lymphocyte Kv1.3 channel. Because KcsA-Kv1.3 protein can be expressed in *Escherichia coli*, this system is amenable to [^{13}C, ^{15}N] isotope labelling, thus far crucial for high-resolution ssNMR studies on proteins (Hughes and Baldus 2005). Compared to the KcsA channel first identified in the gram-positive bacterium *Streptomyces lividans* (Schrempf et al. 1995), KcsA-Kv1.3 differs by 11 amino acids, predominantly found in the pore region of the channel (Legros et al. 2000, 2002) (Fig. 7). For the KcsA system, X-ray structures exist for the transmembrane and extracellular regions (Doyle et al. 1998; Zhou et al. 2001a) (PDB entries: 1BL8, 1J95), for variable potassium concentrations (Zhou et al. 2001b) (PDB: 1K4C, 1K4D) and in the presence of Rb, Tl (Zhou and MacKinnon 2003) (PDB: 1R3J, 1R3J) and TEA (Lenaeus et al. 2005) (PDB: 2BOB,

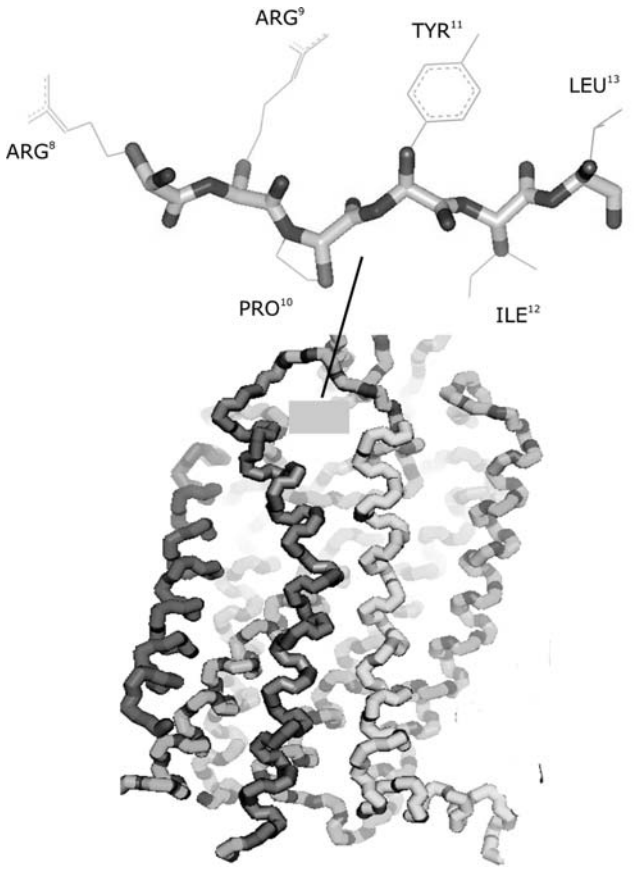

Fig. 6 Backbone ssNMR model of NT(8–13) as determined by Luca et al. (2003) and putative binding site of NT(8–13) involving loop 3 according to (Barroso et al. 2000)

KTX:
GVEINVKCSG SPQCLKPCKD AGMRFGKCMN RKCHCTPK

KcsA-Kv1.3:
MRGSHHHHHHGIR
1 11 21 31 41
MPPMLSGLLARLVKLLLGRHGSALHWRAAGAATVLLVIVLLAGSYLAVLA
51 61 71 81 91
E**ADDP**T**SGFSSI**P**D**ALWWSVETATTVGYGDLYPVTLWGRCVAVVVMVAGI
101 111 121 131 141
TSFGLVTAALATWFVGREQERRGHFVRHSEKAAEEAYTRTTRALHERFDR
151
LERMLDDNRR

Fig. 7 Amino acid sequence of Kaliotoxin (KTX) and the chimeric KcsA-Kv1.3 channel. In the latter case, mutations in reference to wild-type KcsA are indicated in *bold*. The transmembrane part of KcsA-Kv1.3 is *underlined*

2BOC). Structural information on the cytoplasmic domains was obtained by combining X-ray results with EPR data on spin-labeled variants of the full length KcsA channel (Cortes et al. 2001) (PDB: 1F6G).

In a first set of experiments, we determined the structure of the free KTX (Fig. 8) confirming the validity of the general concept using (^{1}H,^{1}H) distances and conformation-dependent chemical shifts to determine 3D polypeptide structures by ssNMR (Lange et al. 2005). Subsequently, a comparison to ssNMR spectra of proteoliposomes containing the free channel and the toxin–ion channel complex allowed us to study the structural rearrangements that are associated with complex formation in a detailed manner. Since the chimeric channel is amendable to isotope labelling, binding was investigated both on the ligand and the channel side. 2D ssNMR of the free, membrane-embedded channel were largely compatible with predictions using the available X-ray structure as reference. In addition, the distinct backbone structure around the active site of the channel facilitated sequential resonance assignments that readily lead to the identification of residue-specific interactions. The corresponding chemical-shift mapping that describes the effect of toxin binding on the level of the channel backbone is shown in Fig. 9 using the KcsA X-ray structure in the conductive state as a reference. Amino acids perturbed by binding are indicated in dark grey, including side chains. These observations strongly suggested that complex formation involves structural rearrangements of the toxin and the selectivity filter of the channel. The latter view not only is in line with structural variations seen upon changes in potassium concentration (Zhou et al. 2001b) and in the presence of Rb, Tl (Zhou and MacKinnon 2003) and TEA (Lenaeus et al. 2005) but also nicely fits to recent X-ray data obtained on KcsA mutants that exhibit distinct structural variations around the selectivity filter (Cordero-Morales et al. 2006). Taking in account molecular plasticity may also be important in future MD-based studies of ligand–ion channel interactions (Yi et al. 2007).

Membrane proteins

While several examples have documented the power of modern ssNMR to study ligand binding to membrane proteins, the determination of entire 3D structures of larger, membrane embedded proteins has thus far been complicated by the length of the amino-acid sequence, the high repetitiveness of hydrophobic residues and the limited spectral resolution due to the dominant influence of a single type of regular (α-helical or β-sheet) secondary structure (Egorova-Zachernyuk et al. 2001; Hiller et al. 2005; van Gammeren et al. 2004). In principle, spectral crowding can be reduced by advanced labelling approaches (see, e.g., Ref. Hiller et al. 2005; Kainosho et al. 2006; van Gammeren et al. 2004), but may be precluded by protein expression levels and/or costs of labelled starting materials.

In a series of experiments, we have recently shown (Etzkorn et al. 2007b) that reverse labelling (Heise et al. 2005a; Vuister et al. 1994) and the application of ssNMR methods that separate spectroscopic signals of mobile,

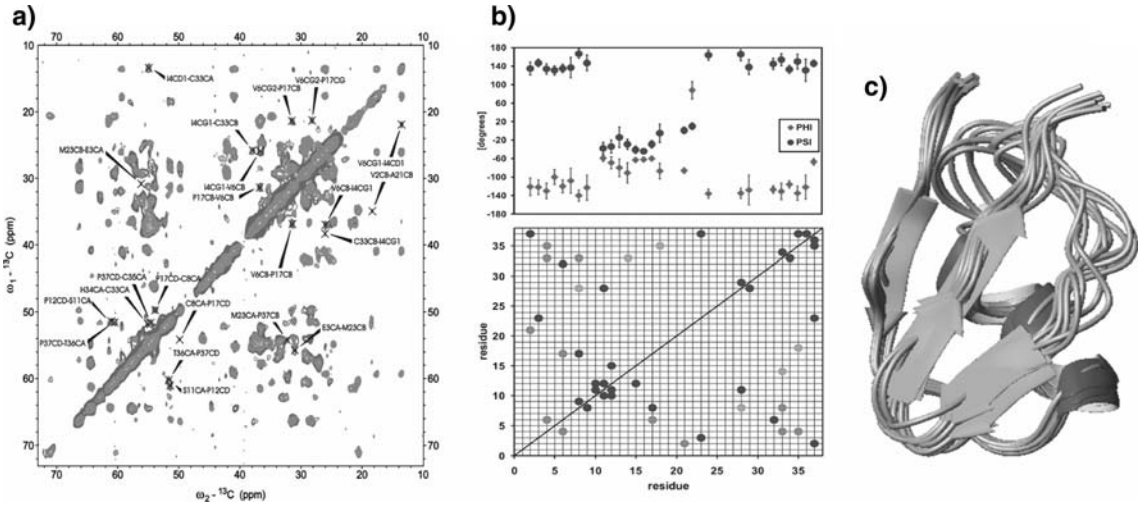

Fig. 8 **a** Overlay of a 2D (^{13}C,^{13}C) spin-diffusion spectrum and a CHHC spectrum of U-[^{13}C,^{15}N]-labeled KTX. Assigned correlations reflect interresidue CHHC constraints. **b** *Top* Dihedral-angle constraints derived from de novo ^{13}C/^{15}N resonance assignments with TALOS (Cornilescu et al. 1999). *Bottom* Interresidue distance CHHC distance restraints and disulfide bonds in KTX. **c** Ribbon diagram of the ten conformers determined by ssNMR spectroscopy with the lowest energy (PDB entry: 1XSW). The conformers were aligned along the backbone by using MOLMOL (Koradi et al. 1996) [adapted from (Lange et al. 2005)]

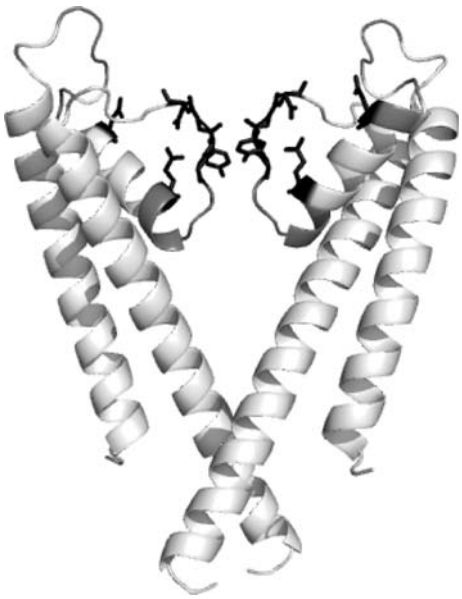

Fig. 9 The effect of KTX binding to the KcsA-Kv1.3 ion channel in lipid bilayers as seen by 2D ssNMR (Lange et al. 2006). Chemical-shift changes were seen for residues indicated in *black* using the KcsA X-ray structure in the conductive state as a reference

static and water-exposed protein segments (see Methods) can be used to monitor structure and topology of an entire seven-helix receptor in native membranes using a single, isotope-labelled sample. Our approach was demonstrated on sensory rhodopsin II from *Natronomonas pharaonis* (NpSRII), a seven-helix (A–G) membrane protein (Klare et al. 2004). 3D structures are available for NpSRII in free (Edman et al. 2002; Luecke et al. 2001; Royant et al. 2001) and transducer bound, ground and light activated form (Gordeliy et al. 2002; Moukhametzianov et al. 2006).

2D ssNMR spectra of a uniformly labelled NpSRII sample that contains four dominant residue types V, L, F, and Y in natural abundance [i.e., U(^{13}C,^{15}N\(V,L,F,Y)) NpSRII] revealed that high-resolution ssNMR spectra can be obtained of membrane proteins in their natural lipid environment. As expected, most signals appearing in dipolar-based correlation experiments arise from the trans-membrane regions of the protein. In Fig. 10, these residues are given in dark grey. On the other hand, through-bond experiments unambiguously revealed that the C-terminus starting from residue 223 onwards is mobile. Additional correlations in the 2D spectra suggest that further protein segments must exhibit high mobility. According to our data, these segments involve loops A–B, B–C and D–E. Indeed, the corresponding secondary chemical shifts of these residues are largely of random-coil character indicative of fast structural rearrangements on the ns to μs time scale. In Fig. 10, these protein segments are given in grey.

Currently, we are comparing these results to crystallographic data and we investigate which structural alterations are taking place in membranes upon formation of the NpSRII/NpHtrII complex.

Conclusions

Thanks to many colleagues in the field, solid-state NMR has made significant progress in studying biological systems in the last years. In this article, I have focused on work

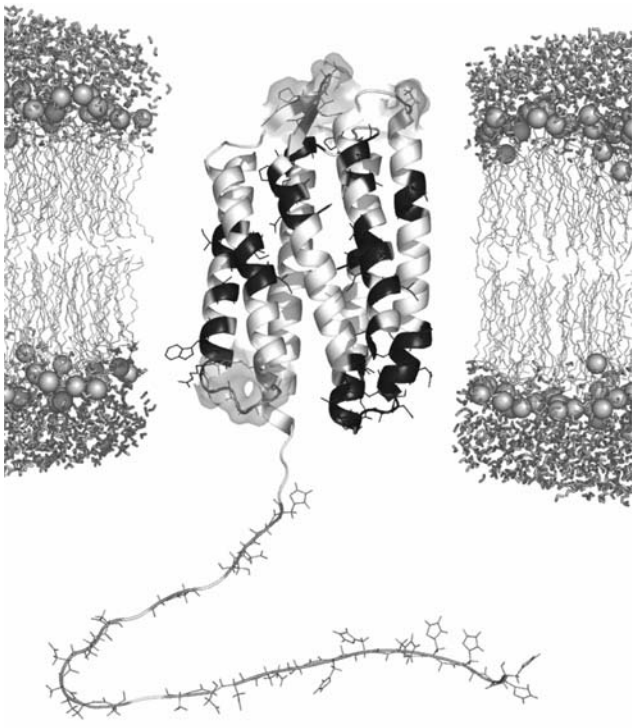

Fig. 10 Graphical representation of the 3D crystal structure of NpSRII in a lipid-bilayer environment. Residues determined by 2D ssNMR as mobile are indicated in *light grey*. Rigid protein segments giving rise to ssNMR correlations are given in *dark grey*

in our group devoted to the study of (membrane) protein structure, folding and ligand binding using multiply-labeled compounds. Progress in ssNMR methodology and instrumentation will further expand the possibilities to study molecular systems of increased size and complexity. In parallel, combination of ssNMR-based approaches with other biophysical and biochemical techniques will increase the level of comprehensiveness with which biological processes such as membrane protein integration or translocation can be studied.

Acknowledgments Work described in this review was supported through grants from the DFG, the FCI, the Volkswagen foundation and the Humboldt foundation, the EU and the Max-Planck Gesellschaft. I thank members of my group and our collaborators over the past 7 years who substantially contributed to work described here. Continuous support by C. Griesinger is gratefully acknowledged.

References

Andrew ER, Bradbury A, Eades RG (1958) Nuclear magnetic resonance spectra from a crystal rotated at high speed. Nature 182:1659

Andronesi OC, Pfeifer JR, Al-Momani L, Özdirekcan S, Rijkers DTS, Angerstein B, Luca S, Koert U, Killian JA, Baldus M (2004) Probing membrane protein structure and orientation under fast magic-angle-spinning. J Biomol NMR 30:253–265

Andronesi OC, Becker S, Seidel K, Heise H, Young HS, Baldus M (2005) Determination of membrane protein structure and dynamics by magic-angle-spinning solid-state NMR spectroscopy. J Am Chem Soc 127:12965–12974

Balbach J, Forge V, Lau WS, van Nuland NAJ, Brew K, Dobson CM (1996) Protein folding monitored at individual residues during a two-dimensional NMR experiment. Science 274:1161–1163

Baldus M (2002) Correlation experiments for assignment and structure elucidation of immobilized polypeptides under magic angle spinning. Prog Nucl Magn Reson Spectrosc 41:1–47

Baldus M (2006) Molecular interactions investigated by multi-dimensional solid-state NMR. Curr Opin Struct Biol 16:618–623

Baldus M, Meier BH (1996) Total correlation spectroscopy in the solid state. The use of scalar couplings to determine the through-bond connectivity. J Mag Res A 121:65–69

Barroso S, Richard F, Nicolas-Etheve D, Reversat JL, Bernassau JM, Kitabgi P, Labbe-Jullie C (2000) Identification of residues involved in neurotensin binding and modeling of the agonist binding site in neurotensin receptor 1. J Biol Chem 275:328–336

Bertoncini CW, Jung Y-S, Fernandez CO, Hoyer W, Griesinger C, Jovin TM, Zweckstetter M (2005) From the cover: release of long-range tertiary interactions potentiates aggregation of natively unstructured a-synuclein. Proc Natl Acad Sci USA 102:1430–1435

Blanco FJ, Tycko R (2001) Determination of polypeptide backbone dihedral angles in solid state NMR by double quantum C−13 chemical shift anisotropy measurements. J Mag Res 149:131–138

Böckmann A, Lange A, Galinier A, Luca S, Giraud N, Heise H, Juy M, Montserret R, Penin F, Baldus M (2003) Solid-state NMR sequential resonance assignments and conformational analysis of the 2*10.4 kDa dimeric form of the bacillus subtilis protein crh. J Biomol NMR 27:323–339

Castellani F, van Rossum B, Diehl A, Schubert M, Rehbein K, Oschkinat H (2002) Structure of a protein determined by solid-state magic-angle-spinning NMR spectroscopy. Nature 420:98–102

Caughey B, Lansbury PT (2003) Protofibrils, pores, fibrils, and neurodegeneration: separating the responsible protein aggregates from the innocent bystanders. Annu Rev Neurosci 26:267–298

Cavanagh J, Fairbrother WJ, Palmer AG, Skelton NJ (1996) Protein NMR spectroscopy, principles and practice. Academic, San Diego

Chan JCC, Oyler NA, Yau WM, Tycko R (2005) Parallel beta-sheets and polar zippers in amyloid fibrils formed by residues 10–39 of the yeast prion protein Ure2p. Biochemistry 44:10669–10680

Chimon S, Ishii Y (2005) Capturing intermediate structures of Alzheimer's Ab (1–40), by solid-state NMR spectroscopy. J Am Chem Soc 127:13472–13473

Conway KA, Harper JD, Lansbury PT (2000) Fibrils formed in vitro from a-synuclein and two mutant forms linked to Parkinson's disease are typical amyloid. Biochemistry 39:2552–2563

Cordero-Morales JF, Cuello LG, Zhao Y, Jogini V, Cortes DM, Roux B, Perozo E (2006) Molecular determinants of gating at the potassium-channel selectivity filter. Nat Struct Mol Biol 13:311–318

Cornilescu G, Delaglio F, Bax A (1999) Protein backbone angle restraints from searching a database for chemical shift and sequence homology. J Biomol NMR 13:289–302

Cortes DM, Cuello LG, Perozo E (2001) Molecular architecture of full-length KcsA: role of cytoplasmic domains in ion permeation and activation gating. J Gen Physiol 117:165–180

Costa PR, Gross JD, Hong M, Griffin RG (1997) Solid-state NMR measurement of Psi in peptides: a NCCN 2Q- heteronuclear local field experiment. Chem Phys Lett 280:95–103

Coutant J, Curmi PA, Toma F, Monti JP (2007) NMR solution structure of neurotensin in membrane-mimetic environments: molecular basis for neurotensin receptor recognition. Biochemistry (in press)

Creemers AFL, Kiihne S, Bovee-Geurts PHM, DeGrip WJ, Lugtenburg J, de Groot HJM (2002) H−1 and C−13 MAS NMR evidence for pronounced ligand–protein interactions involving the ionone ring of the retinylidene chromophore in rhodopsin. Proc Natl Acad Sci USA 99:9101–9106

Creuzet F, McDermott A, Gebhard R, Vanderhoef K, Spijkerassink MB, Herzfeld J, Lugtenburg J, Levitt MH, Griffin RG (1991) Determination of membrane–protein structure by rotational resonance NMR—bacteriorhodopsin. Science 251:783–786

Cross TA, Opella SJ (1994) Solid-state NMR structural studies of peptides and proteins in membranes. Curr Opin Struct Biol 4:574–581

Cross TA, Frey MH, Opella SJ (1983) 15N spin exchange in a protein. J Am Chem Soc 105:7471–7473

Dobson CM (2002) Protein-misfolding diseases: getting out of shape. Nature 418:729–730

Doyle DA, Cabral JM, Pfuetzner RA, Kuo AL, Gulbis JM, Cohen SL, Chait BT, MacKinnon R (1998) The structure of the potassium channel: molecular basis of K+ conduction and selectivity. Science 280:69–77

Dyson HJ, Wright PE (2004) Unfolded proteins and protein folding studied by NMR. Chem Rev 104:3607–3622

Edman K, Royant A, Nollert P, Maxwell CA, Pebay-Peyroula E, Navarro J, Neutze R, Landau EM (2002) Early structural rearrangements in the photocycle of an integral membrane sensory receptor. Structure 10:473–482

Egorova-Zachernyuk TA, Hollander J, Fraser N, Gast P, Hoff AJ, Cogdell R, de Groot HJM, Baldus M (2001) Heteronuclear 2D-correlations in a uniformly [C−13, N−15] labeled membrane–protein complex at ultra-high magnetic fields. J Biomol NMR 19:243–253

Eilers M, Ying WW, Reeves PJ, Khorana HG, Smith SO (2002) Magic angle spinning nuclear magnetic resonance of isotopically labeled rhodopsin. Methods Enzymol 343:212–222

Ernst RR, Bodenhausen G, Wokaun A (1987) Principles of nuclear magnetic resonance in one and two dimensions. Clarendon, Oxford

Etzkorn M, Bockmann A, Penin F, Riedel D, Baldus M (2007a) Characterization of folding intermediates of a domain-swapped protein by solid-state NMR spectroscopy. J Am Chem Soc 129:169–175

Etzkorn M, Martell S, Andronesi Ovidiu C, Seidel K, Engelhard M, Baldus M (2007b) Secondary structure, dynamics, and topology of a seven-helix receptor in native membranes, studied by solid-state NMR spectroscopy. Angewandte Chem Int 46:459–462

Feng X, Verdegem PJE, Lee YK, Sandstrom D, Eden M, BoveeGeurts P, deGrip WJ, Lugtenburg J, deGroot HJM, Levitt MH (1997) Direct determination of a molecular torsional angle in the membrane protein rhodopsin by solid-state NMR. J Am Chem Soc 119:6853–6857

Ferguson N, Becker J, Tidow H, Tremmel S, Sharpe TD, Krause G, Flinders J, Petrovich M, Berriman J, Oschkinat H, Fersht AR (2006) General structural motifs of amyloid protofilaments. Proc Natl Acad Sci USA 103:16248–16253

van Gammeren AJ, Hulsbergen FB, Hollander JG, de Groot HJM (2004) Biosynthetic site-specific C-13 labeling of the light-harvesting 2 protein complex: a model for solid state NMR structure determination of transmembrane proteins. J Biomol NMR 30:267–274

Glaubitz C, Watts A (1998) Magic angle-oriented sample spinning (MAOSS): a new approach toward biomembrane studies. J Mag Res 130:305–316

Goedert M (1989) Radioligand-binding assays for study of neurotensin receptors. Methods Enzymol 168:462–481

Gordeliy VI, Labahn J, Moukhametzianov R, Efremov R, Granzin J, Schlesinger R, Buldt G, Savopol T, Scheidig AJ, Klare JP, Engelhard M (2002) Molecular basis of transmembrane signalling by sensory rhodopsin II-transducer complex. Nature 419:484–487

Griffin RG (1981) Solid state nuclear magnetic resonance of lipid bilayers. Methods Enzymol 72:108–174

Griffin RG (1998) Dipolar recoupling in MAS spectra of biological solids. Nat Struct Biol 5:508–512

Grisshammer R, Tucker J (2000) Expression in *Escherichia coli* and large-scale purification of a rat neurotensin receptor. In: Haga T, Bernstein G (eds) G protein coupled receptors. CRC, Boca Raton, pp 265–280

de Groot HJM (2000) Solid-state NMR spectroscopy applied to membrane proteins. Curr Opin Struct Biol 10:593–600

Havlin RH, Tycko R (2005) Probing site-specific conformational distributions in protein folding with solid-state NMR. Proc Natl Acad Sci USA 102:3284–3289

Heise H, Hoyer W, Becker S, Andronesi OC, Riedel D, Baldus M (2005a) Molecular-level secondary structure, polymorphism, and dynamics of full-length {alpha}-synuclein fibrils studied by solid-state NMR. Proc Natl Acad Sci USA 102:15871–15876

Heise H, Luca S, de Groot BL, Grubmuller H, Baldus M (2005b) Probing conformational disorder in neurotensin by two-dimensional solid-state NMR and comparison to molecular dynamics simulations. Biophys J 89:2113–2120

Heise H, Seidel K, Etzkorn M, Becker S, Baldus M (2005c) 3D Spectroscopy for resonance assignment and structure elucidation of proteins under MAS: novel pulse schemes and sensitivity considerations. J Mag Res 173:64–74

Heise H, Hoyer W, Becker S, Seidel K, Baldus M (2007) Fibril topology of full-length a-synuclein probed by solid-state NMR spectroscopy (submitted)

Herzfeld J, Lansing JC (2002) Magnetic resonance studies of the bacteriorhodopsin pump cycle. Annu Rev Biophys Biomol Struct 31:73–95

Hiller M, Krabben L, Vinothkumar KR, Castellani F, van Rossum BJ, Kuhlbrandt W, Oschkinat H (2005) Solid-state magic-angle spinning NMR of outer-membrane protein G from *Escherichia coli*. Chembiochem 6:1679–1684

Hong M (2006) Oligomeric structure, dynamics, and orientation of membrane proteins from solid-state NMR. Structure 14:1731–1740

Hong M, Gross JD, Griffin RG (1997) Site-resolved determination of peptide torsion angle phi from the relative orientations of backbone N–H and C–H bonds by solid-state NMR. J Phys Chem B 101:5869–5874

Hughes CE, Baldus M (2005) Magic-angle-spinning solid-state NMR applied to polypeptides and proteins. Ann Rep NMR Spect 55:121–158

Inooka H, Ohtaki T, Kitahara O, Ikegami T, Endo S, Kitada C, Ogi K, Onda H, Fujino M, Shirakawa M (2001) Conformation of a peptide ligand bound to its G-protein coupled receptor. Nature Struct Bio 8:161–165

Ishii Y, Terao T, Kainosho M (1996) Relayed anisotropy correlation NMR: determination of dihedral angles in solids. Chem Phys Lett 256:133–140

Iwata K, Fujiwara T, Matsuki Y, Akutsu H, Takahashi S, Naiki H, Goto Y (2006) 3D structure of amyloid protofilaments of b2-microglobulin fragment probed by solid-state NMR. Proc Natl Acad Sci USA103:18119–18124

Jaroniec CP, Tounge BA, Herzfeld J, Griffin RG (2001) Frequency selective heteronuclear dipolar recoupling in rotating solids: Accurate C–13–N-15 distance measurements in uniformly C−13,N−15-labeled peptides. J Am Chem Soc 123:3507–3519

Jaroniec CP, MacPhee CE, Bajaj VS, McMahon MT, Dobson CM, Griffin RG (2004) High-resolution molecular structure of a peptide in an amyloid fibril determined by magic angle spinning NMR spectroscopy. Proc Natl Acad Sci USA 101:711–716

Kainosho M, Torizawa T, Iwashita Y, Terauchi T, Mei Ono A, Güntert P (2006) Optimal isotope labelling for NMR protein structure determinations. Nature 440:52–57

Klare JP, Gordeliy VI, Labahn J, Büldt G, Steinhoff H-J, Engelhard M (2004) The archaeal sensory rhodopsin II/transducer complex: a model for transmembrane signal transfer. FEBS Lett 564:219–224

Koradi R, Billeter M, Wuthrich K (1996) MOLMOL: a program for display and analysis of macromolecular structures. J Mol Graph 14:51–55

Krabben L, van Rossum BJ, Castellani F, Bocharov E, Schulga AA, Arseniev AS, Weise C, Hucho F, Oschkinata H (2004) Towards structure determination of neurotoxin II bound to nicotinic acetylcholine receptor: a solid-state NMR approach. FEBS Lett 564:319–324

Kumashiro KK, Schmidt-Rohr K, Murphy OJ, Ouellette KL, Cramer WA, Thompson LK (1998) A novel tool for probing membrane protein structure: solid-state NMR with proton spin diffusion and X-nucleus detection. J Am Chem Soc 120:5043–5051

Ladizhansky V, Jaroniec CP, Diehl A, Oschkinat H, Griffin RG (2003) Measurement of multiple psi torsion angles in uniformly C−13,N−15-labeled alpha-spectrin SH3 domain using 3D N-15-C-13-C-13-N-15 MAS dipolar-chemical shift correlation spectroscopy. J Am Chem Soc 125:6827–6833

Lange A, Luca S, Baldus M (2002) Structural constraints from proton-mediated rare-spin correlation spectroscopy in rotating solids. J Am Chem Soc 124:9704–9705

Lange A, Seidel K, Verdier L, Luca S, Baldus M (2003) Analysis of proton–proton transfer dynamics in rotating solids and their use for 3D structure determination. J Am Chem Soc 125:12640–12648

Lange A, Becker S, Seidel K, Giller K, Pongs O, Baldus M (2005) A concept for rapid protein-structure determination by solid-state NMR spectroscopy. Angew Chem Int Ed 44:2089–2092

Lange A, Giller K, Hornig S, Martin-Eauclaire M-F, Pongs O, Becker S, Baldus M (2006) Toxin-induced conformational changes in a potassium channel revealed by solid-state NMR. Nature 440:959–962

Legros C, Pollmann V, Knaus HG, Farrell AM, Darbon H, Bougis PE, Martin-Eauclaire MF, Pongs O (2000) Grenerating a high affinity scorpion toxin receptor in KcsA- Kv1.3 chimeric potassium channels. J Biol Chem 275:16918–16924

Legros C, Schulze C, Garcia ML, Bougis PE, Martin-Eauclaire MF, Pongs O (2002) Engineering-specific pharmacological binding sites for peptidyl inhibitors of potassium channels into KcsA. Biochemistry 41:15369–15375

Lenaeus MJ, Vamvouka M, Focia PJ, Gross A (2005) Structural basis of TEA blockade in a model potassium channel. Nat Struct Mol Biol 12:454–459

Luca S, White JF, Sohal AK, Filippov DV, van Boom JH, Grisshammer R, Baldus M (2003) The conformation of neurotensin bound to its G protein-coupled receptor. Proc Natl Acad Sci USA 100:10706–10711

Luca S, Lange A, Heise H, Baldus M (2005) Investigation of ligand–receptor interactions by high-resolution solid-state NMR. Arch Pharm (Weinheim) 338:217–228

Luecke H, Schobert B, Lanyi JK, Spudich EN, Spudich JL (2001) Crystal structure of sensory rhodopsin II at 2.4 Angstroms: insights into color tuning and transducer interaction. Science 293:1499–1503

Makin OS, Atkins E, Sikorski P, Johansson J, Serpell LC (2005) Molecular basis for amyloid fibril formation and stability. Proc Natl Acad Sci USA 102:315–320

Marassi FM, Opella SJ (1998) NMR structural studies of membrane proteins. Curr Opin Struct Biol 8:640–648

McDermott AE (2004) Structural and dynamic studies of proteins by solid-state NMR spectroscopy: rapid movement forward. Curr Opin Struct Biol 14:554–561

McDowell LM, Schaefer J (1996) High-resolution NMR of biological solids. Curr Opin Struct Biol 6:624–629

Morris GA, Freeman R (1979) Enhancement of nuclear magnetic-resonance signals by polarization transfer. J Am Chem Soc 101:760–762

Moukhametzianov R, Klare JP, Efremov R, Baeken C, Gäppner A, Labahn Jr, Engelhard M, Büldt G, Gordeliy VI (2006) Development of the signal in sensory rhodopsin and its transfer to the cognate transducer. Nature 440:115–119

Nelson R, Sawaya MR, Balbirnie M, Madsen AO, Riekel C, Grothe R, Eisenberg D (2005) Structure of the cross-b spine of amyloid-like fibrils. Nature 435:773–778

Nomura K, Takegoshi K, Terao T, Uchida K, Kainosho M (1999) Determination of the complete structure of a uniformly labeled molecule by rotational resonance solid-state NMR in the tilted rotating frame. J Am Chem Soc 121:4064–4065

Opella SJ (1986) Protein dynamics by solid state nuclear magnetic resonance. Methods Enzymol 131:327–361

Opella SJ, Marassi FM (2004) Structure determination of membrane proteins by NMR spectroscopy. Chem Rev 104:3587–3606

Palmer AG, Williams J, McDermott A (1996) Nuclear magnetic resonance studies of biopolymer dynamics. J Phys Chem 100:13293–13310

Patel AB, Crocker E, Eilers M, Hirshfeld A, Sheves M, Smith SO (2004) Coupling of retinal isomerization to the activation of rhodopsin. Proc Natl Acad Sci USA 101:10048–10053

Petkova AT, Ishii Y, Balbach JJ, Antzutkin ON, Leapman RD, Delaglio F, Tycko R (2002) A structural model for Alzheimer's b-amyloid fibrils based on experimental constraints from solid state NMR. Proc Natl Acad Sci USA 99:16742–16747

Petkova AT, Buntkowsky G, Dyda F, Leapman RD, Yau WM, Tycko R (2004) Solid state NMR reveals a pH-dependent antiparallel b-sheet registry in fibrils formed by a b-amyloid peptide. J Mol Biol 335:247–260

Petkova AT, Leapman RD, Guo Z, Yau W-M, Mattson MP, Tycko R (2005) Self-propagating, molecular-level polymorphism in Alzheimer's b-amyloid fibrils. Science 307:262–265

Petkova AT, Yau WM, Tycko R (2006) Experimental constraints on quaternary structure in Alzheimer's b-amyloid fibrils. Biochemistry 45:498–512

Reif B, Hohwy M, Jaroniec CP, Rienstra CM, Griffin RG (2000) NH–NH vector correlation in peptides by solid-state NMR. J Mag Res 145:132–141

Rienstra CM, Hohwy M, Mueller LJ, Jaroniec CP, Reif B, Griffin RG (2002) Determination of multiple torsion-angle constraints in U-C- 13,N-15-labeled peptides: 3D H-1-N-15-C-13-H-1 dipolar chemical shift NMR spectroscopy in rotating solids. J Am Chem Soc 124:11908–11922

Ritter C, Maddelein M-L, Siemer AB, Lührs T, Ernst M, Meier BH, Saupe SJ, Riek R (2005) Correlation of structural elements and infectivity of the HET-s prion. Nature 435:844–848

Royant A, Nollert P, Edman K, Neutze R, Landau EM, Pebay-Peyroula E, Navarro J (2001) X-ray structure of sensory rhodopsin II at 2.1-A resolution. Proc Natl Acad Sci USA 98:10131–10136

Schneider R, Etzkorn M, Baldus M (2007) Molecular motion detected by double-quantum (13C,13C) solid-state NMR spectroscopy (submitted)

Schrempf H, Schmidt O, Kummerlen R, Hinnah S, Muller D, Betzler M, Steinkamp T, Wagner R (1995) A prokaryotic potassium-ion channel with 2 predicted transmembrane segments from *Streptomyces lividans*. EMBO J 14:5170–5178

Seidel K, Lange A, Becker S, Hughes CE, Heise H, Baldus M (2004) Protein solid-state NMR resonance assignments from (13C,13C) correlation spectroscopy. PhysChemChemPhys 6:5090–5093

Seidel K, Etzkorn M, Sonnenberg L, Griesinger C, Sebald A, Baldus M (2005) Studying 3D structure and dynamics by high-resolution

solid-state NMR: application to L-tyrosine–ethylester. J Phys Chem A 109:2436–2442
Serpell LC, Berriman J, Jakes R, Goedert M, Crowther RA (2000) Fiber diffraction of synthetic a-synuclein filaments shows amyloid-like cross-b conformation. Proc Natl Acad Sci USA 97:4897–4902
Shewmaker F, Wickner RB, Tycko R (2006) Amyloid of the prion domain of Sup35p has an in-register parallel b-sheet structure. Proc Natl Acad Sci USA 103:19754–19759
Siemer AB, Arnold AA, Ritter C, Westfeld T, Ernst M, Riek R, Meier BH (2006) Observation of highly flexible residues in amyloid fibrils of the HET-s prion. J Am Chem Soc 128:13224–13228
Sizun C, Bechinger B (2002) Bilayer sample for fast or slow magic angle oriented sample spinning solid-state NMR spectroscopy. J Am Chem Soc 124:1146–1147
Sonnenberg L, Luca S, Baldus M (2004) Multiple-spin analysis of (13C,13C) chemical-shift selective transfer in uniformly labeled biomolecules. J Mag Res 166:100–110
Sunde M, Serpell LC, Bartlam M, Fraser PE, Pepys MB, Blake CCF (1997) Common core structure of amyloid fibrils by synchrotron X-ray diffraction. J Mol Biol 273:729–739
Tanaka K, Masu M, Nakanishi S (1990) Structure and functional expression of the cloned rat neurotensin receptor. Neuron 4:847–854
Torchia DA (1984) Solid-state NMR-studies of protein internal dynamics. Annu Rev Biophys Bioeng 13:125–144
Tycko R (2004) Progress towards a molecular-level structural understanding of amyloid fibrils. Curr Opin Struct Biol 14:96–103
Tycko R (2006) Molecular Structure of amyloid fibrils: insights from solid-state NMR. Quart Rev Biophys 39:1–55
vanderWel PCA, Hu KN, Lewandowski J, Griffin RG (2006) Dynamic nuclear polarization of amyloidogenic peptide nanocrystals: GNNQQNY, a core segment of the yeast prion protein Sup35p. J Am Chem Soc 128:10840–10846
Vuister GW, Kim SJ, Wu C, Bax A (1994) 2d and 3d NMR-study of phenylalanine residues in proteins by reverse isotopic labeling. J Am Chem Soc 116:9206–9210
Watts A (1999) NMR of drugs and ligands bound to membrane receptors. Curr Opin Biotechnol 10:48–53
Watts A (2005) Solid-state NMR in drug design and discovery for membrane-embedded targets. Nature Rev Drug Disc 4:555–568
Weinreb PH, Zhen WG, Poon AW, Conway KA, Lansbury PT (1996) NACP, a protein implicated in Alzheimer's disease and learning, is natively unfolded. Biochemistry 35:13709–13715
Williamson PTF, Bains S, Chung C, Cooke R, Watts A (2002) Probing the environment of neurotensin whilst bound to the neurotensin receptor by solid-state NMR. FEBS Lett 518:111–115
Wishart DS, Sykes BD (1994) Chemical-shifts as a tool for structure determination. Nucl Magn Reson Pt C 239:363–392
Wüthrich K (1986) NMR of proteins and nucleic acids. Wiley Interscience, New York
Yi H, Cao ZJ, Yin SJ, Dai C, Wu YL, Li WX (2007) Interaction simulation of hERG K+ channel with its specific BeKm−1 peptide: insights into the selectivity of molecular recognition. J Prot Res 6:611–620
Zhou M, Morais-Cabral JH, Mann S, MacKinnon R (2001a) Potassium channel receptor site for the inactivation gate and quaternary amine inhibitors. Nature 411:657–661
Zhou YF, Morais-Cabral JH, Kaufman A, MacKinnon R (2001b) Chemistry of ion coordination and hydration revealed by a K+ channel-Fab complex at 2.0 Angstrom resolution. Nature 414:43–48
Zhou Y, MacKinnon R (2003) The occupancy of ions in the K+ selectivity filter: charge balance and coupling of ion binding to a protein conformational change underlie high conduction rates. J Mol Biol 333:965–975